Technology Collaboration Programme
by iea

International Energy Agency
Photovoltaic Power Systems Programme

Task 17: PV and Transport

PVPS

Irradiance and Temperature Uniformity on Vehicle Roof

2025

Report IEA-PVPS T17-05:2025

What is IEA PVPS TCP?

The International Energy Agency (IEA), founded in 1974, is an autonomous body within the framework of the Organization for Economic Cooperation and Development (OECD). The Technology Collaboration Programme (TCP) was created with a belief that the future of energy security and sustainability starts with global collaboration. The programme is made up of 6 000 experts across government, academia, and industry dedicated to advancing common research and the application of specific energy technologies.

The IEA Photovoltaic Power Systems Programme (IEA PVPS) is one of the TCP's within the IEA and was established in 1993. The mission of the programme is to "enhance the international collaborative efforts which facilitate the role of photovoltaic solar energy as a cornerstone in the transition to sustainable energy systems." In order to achieve this, the Programme's participants have undertaken a variety of joint research projects in PV power systems applications. The overall programme is headed by an Executive Committee, comprised of one delegate from each country or organisation member, which designates distinct 'Tasks,' that may be research projects or activity areas.

The IEA PVPS participants Australia, Austria, Belgium, Canada, China, Denmark, Enercity SA, European Union, Finland, France, Germany, India, Israel, Italy, Japan, Korea, Malaysia, Morocco, the Netherlands, Norway, Portugal, Solar Energy Research Institute of Singapore (SERIS), SolarPower Europe, South Africa, Spain, Sweden, Switzerland, Thailand, Turkey, United States..

Visit us at: www.iea-pvps.org

What is IEA PVPS Task 17?

The objective of Task 17 of the IEA Photovoltaic Power Systems Programme is to deploy PV in the transport, which will contribute to reducing CO_2 emissions of the transport and enhancing PV market expansions. The results contribute to clarifying the potential of utilization of PV in transport and to propose how to proceed toward realising the concepts.

Task 17's scope includes PV-powered vehicles such as PLDVs (passenger light duty vehicles), LCVs (light commercial vehicles), HDVs (Heavy Duty Vehicles) and other vehicles, as well as PV applications for electric systems and infrastructures, such as charging infrastructure with PV, battery and other power management systems.

Authors

- **Bertrand Chambion, Shehrazade Nassibi, Lionel Serra, Aurélien Raddenzati, Ya-Brigitte Assoa**

COVER PICTURE

VIPV roof prototype, CEA-INES

INTERNATIONAL ENERGY AGENCY

PHOTOVOLTAIC POWER SYSTEMS PROGRAMME

IEA PVPS
Task 17
PV and Transport

Irradiance and Temperature Uniformity on Vehicle Roof

Report IEA-PVPS T17-05:2025
January 2025

TABLE OF CONTENTS

ACKNOWLEDGMENT

This paper has received valuable contributions from several IEA-PVPS Task 17 members and other international experts. Many thanks to all of them.

The French contribution is funded by the Agency for Ecological Transition (ADEME) under grant number 1905C0043 (PV2E-Mobility).

This work is part of the development of photovoltaic integration in transport (VIPV) and is part of the TI-PV project funded by ADEME, the French Environment and Energy Management Agency.

LIST OF ABBREVIATIONS

AC	Alternating Current
DC	Direct Current
EV	Electric Vehicle
GHG	Greenhouse Gas
IIREVs	Intelligent Infrastructure Recharging Electric Vehicles
MG	MicroGrid
MPPT	Maximum Power Point Tracking
PV	PhotoVoltaic
PVCS	PV-powered Charging Station
SOC	State of Charge
UTC	Université de Technologie de Compiègne
V2B	Vehicle-to-Building
V2G	Vehicle-to-Grid
V2H	Vehicle-to-home
V2V	Vehicle-to-Vehicle
V2X	Vehicle-to-Everything
VIPV	Vehicle Integrated Photovoltaic

LIST OF TABLES

LIST OF FIGURES

EXECUTIVE SUMMARY

In the transport sector, battery and plug-in hybrid electric vehicles are being adopted globally as a solution to mitigate CO_2 emissions. In line with this, vehicle emissions targets have been proposed and adopted by many countries and policy bodies around the world with goals for the adoption and use of electric vehicles in the near future. With widespread electrification of transportation, PV generated electricity and other renewable energy sources are needed to leverage the EV adoption into even more significant CO_2 emissions reductions. The distributed nature of PV electricity generation offers new opportunities for charging battery electric vehicles.

Options for low-carbon charging of electric vehicles include charging from the existing grid network with PV or other sustainable electricity sources, charging from a dedicated charge point with local PV electricity generation, or directly and independently with on-board PV (PV-powered vehicle). In order to contribute to reducing the CO_2 emissions of the transport sector and to enhance PV market expansions, IEA PVPS Task 17 is aiming to clarify the potential of the utilization of PV in transport and to propose how to proceed towards realising the concepts. Task 17's scope includes various PV-powered vehicles such as passenger vehicles, light commercial vehicles, heavy duty vehicles and other vehicles, as well as PV applications for electric systems and infrastructures, such as charging infrastructure with PV, battery and other power management systems.

This report is aimed at potential integrators of curved solar surfaces on vehicles, whether for setting up an experimental solar irradiation and temperature monitoring system on curved surface (chapters 2 to 4) or for energy assessment due to curvature (chapter 5 and conclusion).

Among these options, this report has focused on PV-powered vehicles, with on-board integrated PV systems (VIPV). A VIPV system can be described as a combination between a PV surface, integrated in the car body, a specific electronic system and on board Energy Management System (EMS), linked to a storage element for PV energy. Most of the time, the main characteristic of the PV element is the peak power (Wp) under standard irradiance (1000 W/m², AM1.5 @25°C). This is a key parameter to predict the solar energy we can get and use from the sun each year. As the PV surface is not flat, but curved in a car solar roof, mismatches appear in term of irradiance and cells temperature. It results in energy losses due to non-uniformity in light incidence angle over the module surface.

This work presents the conceptualization of an instrumented roof equipped with irradiance and temperature sensors. The aim of this report is to outline the manufacturing stages on a vehicle roof, from cell selection to module assembly, and finally to assembly of the outdoor monitoring system. As a curved roof induce losses due to PV exposition mismatches, we propose to measure, directly on real vehicle roof, irradiance and temperature homogeneity, thanks to a 5x5 individual sensor matrix coupled to a specific data logger configuration on a 1.4*0.9 m² vehicle roof. Two options were investigated: using photodiodes or existing solar cells as irradiance sensor. Due to representative surface of real cells and light collection in a module structure, individual solar cells are used. This study, over 8 days during August 2023, recorded target parameters in Le Bourget du Lac, France. For clear sunny days, Irradiance data reveals up to 250 W/m² (21%) difference between best and worst oriented cell on the roof. Regarding temperature, up to 13 °C difference is confirmed. For rainy days, we found less than 20 W/m² irradiance difference and less than 3 °C temperature homogeneity. These results are summarized in the figure below. Thus, we propose to consider irradiance and temperature mismatches only on clear sky conditions (direct irradiance as main energy contribution). These conclusions will be tested in our energy prediction model at vehicle level to estimate the accuracy/complexity of this approach.

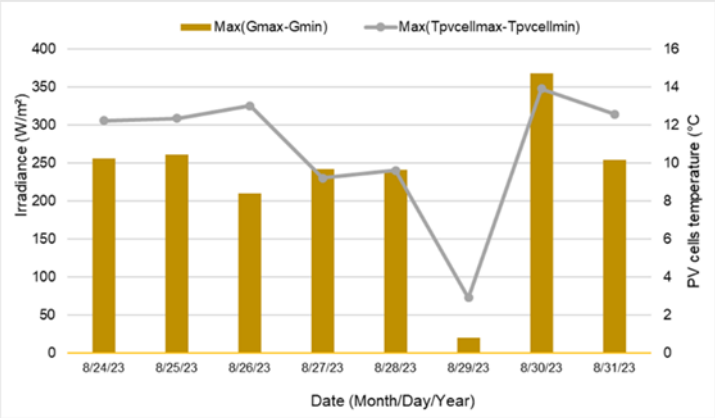

Delta values	Max(Gmax-Gmin) (W/m²)	Max(Tpvcellmax-Tpvcellmin) (°C)
8/24/2023	255,67	**12,22**
8/25/2023	261,04	**12,33**
8/26/2023	210,00	**13,00**
8/27/2023	242,07	**9,19**
8/28/2023	240,16	**9,59**
8/29/2023	19,58	**2,89**
8/30/2023	367,27	**13,89**
8/31/2023	254,07	**12,55**

Maximum values for irradiance homogeneity and cell temperature on solar roof over experiment time. It focuses only on maximum values

This report illustrated the various stages in the implementation of a measurement bench, from design, installation, monitoring phase and data processing, recorded during 8 days, during August 2023, at INES site, Le Bourget du Lac, France.

A simple theoretical comparison confirmed that irradiance and temperature uniformity is mainly due to roof curvature. Energy calculations coupled with a full serial cells connection hypothesis and a curved surface (Radius of curvature =3 m) show that the energy harvesting is limited by 12% to 17% performance loss on clear sky sunny day, and 6% for rainy days. These values are valid for August, at Le Bourget du Lac, France, only.

This study should be done on one-year duration to collect representative datas. Further steps will focus on energy model prediction at vehicle level (irradiance and temperature mismatch versus standard “x” % losses approach) to quantify the accuracy/complexity of both approaches. Another interesting work should be to install again this bench over a year to duplicate this study on several location.

1- INTRODUCTION

Solar module performance is directly dependent on irradiance and temperature. In the case of the VIPV, we are interested in the impact that a curvature can have on the uniformity of irradiance received on the vehicle roof.

To answer this question, we decided to build an instrumented solar roof incorporating a number of temperature and solar irradiance sensors. The solar roof is designed on a vehicle roof and is directly linked to a data collection system. Measurements are taken outdoors in an unshaded area.

One of the main objectives of the test bench is to retrieve some irradiance and temperature data from typical summer weathers on a curved roof of a vehicle. This experiment has been setup on an area with no shading in order to record only the influence of the curvature of car roof. The system has been settled on southern exposition. A correlation is expected between the curvature and the irradiance measurement. A further data processing will extract the irradiance mapping during three different scenarios:

- One scorching clear summer day.
- One cloudy day.
- One rainy day with temperature below the seasonal norm.

The tests lasted a full week with all the sun positions during week 34, August 2023 in Bourget du Lac (France). All the three scenarios were able to be recorded during this week.

Each detector has been paired with a thermocouple wire to map the temperature profile of the roof exposed to full sun.

2- EXPERIMENTAL METHODOLOGY

2.1 Tests bench specifications

The main objective is to map the irradiance of a curved roof during bright and cloudy days. The systems have to contain enough data in order to map the full surface of the structure. We needed to define how many detectors have to be set to get a sufficient mapping of the roof. The channels of the available datalogger limit this number. Indeed, the maximum is fixed to 50 measurements with 25 irradiance values and 25 temperatures. Therefore, we had to cover the irradiance matrix measurement along the roof surface with a 5x5 matrix.

Another important parameter is the acquisition frequency. Due to this large number of detectors, a compromise had to be defined.

Therefore, we can list all the specifications needed for the irradiance matrix measurements:

- Irradiance kit has to be flexible to fit the curve of the car roof. A lightweight, easy to fold structure of the kit is mandatory to highlight the curvature dependency of the illumination of the non-plane surface.
- Number of detectors should be representative to get enough data for squaring the irradiance measured on the car roof.
- This number should not exceed 50 connectors due to the limitation of the datalogger used in this protocol.
- The car roof has to be in a clear area with no shade. Indeed, partial shading effects are not desired in this study. These add more complexifications of the interpretation and this will be another subject to pursue.
- Datalogger acquisition frequency has to be representative as well. We set the measurement at one full acquisition every minute.

Two solution were considered for fitting the specification listed above:

- One matrix of commercial photodiodes
- One matrix with solar ½ M6 solar cells

Both of these solutions present some advantages and inconvenient that we are going to describe in the following section.

2.2 Solution envisaged for the design of the measuring bench

2.2.1 Using a photodiode as an illumination sensor

The first concept considered to fit the irradiance kit specification was to map the solar roof with commercial photodiode matrix. We selected The Silicon PIN Photodiode VEMD5080X01 from Vishay Semiconductors [1] whose physical specifications was the best matched for the conception of the bench design.

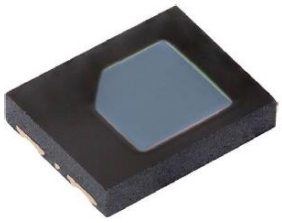

Figure 1: PIN Photodiode VEMD5080X01 from Vishay Semiconductors.

This photodiode is a SMD (surface mounted device) component with a sensitive surface of 7.5 mm². The dimension is: 5 mm x 4 mm x 0.9 mm (L x W x H). A printed circuit is needed to use this photodiode.

One solution is to pave the car roof with commercial photodiodes. Some PIN photodiodes were tested on a test board with a dedicated resistance (from datasheet). Its value was chosen to fit the system: 1k2 ohm. The printed circuit designed is presented on Figure 2.

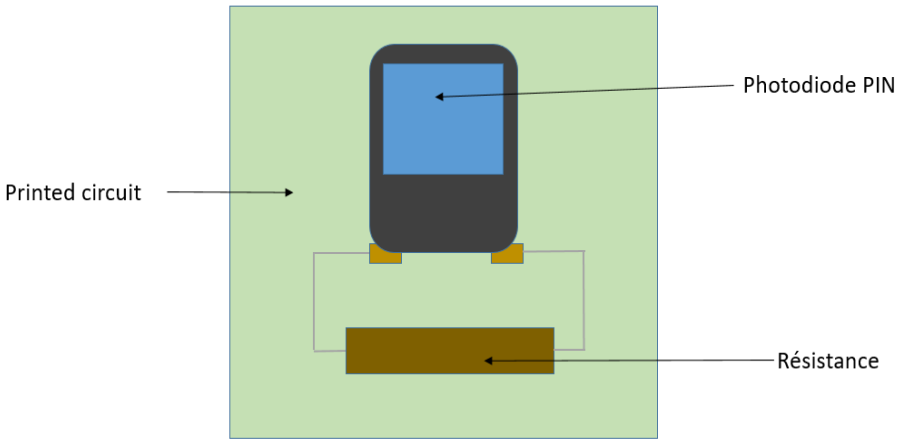

Figure 2: Simplified illustration of the photodiode and resistor assembly on an electronic circuit.

Other features were also considered: the relative spectral sensitivity and the angular displacement. The photodiode is silicon-based component so all the solar spectrum from 400 nm and 1100 nm is converted with a peak of sensitivity at 950 nm. The spectral response fit the specification of the tests bench. Furthermore, the angular displacement is also needed to be taken into account. Indeed, solar sun position sweep from -90° to 90° on the component from dawn to dusk and the angular sensitivity change along the daytime. We can apply a multiplicative factor to fix the lack of sensitivity at early morning and late evening. The two photodiodes specification is illustrated on Figures 3 and 4.

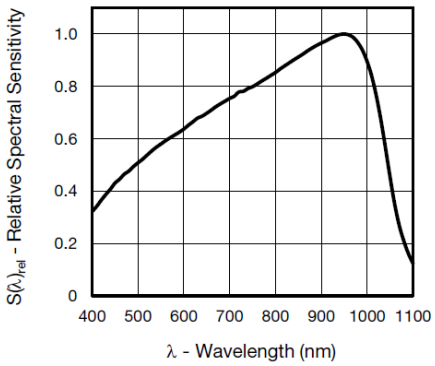

Figure 4: Relative Spectral Sensitivity vs. Wavelength

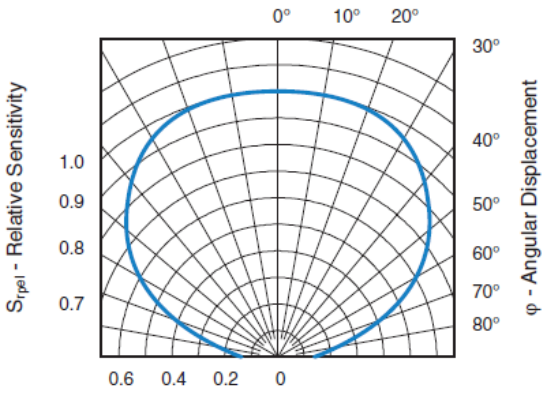

Figure 3: Relative Sensitivity vs. Angular Displacement.

A system of 3 photodiodes with resistance were tested on an electronic test board (Figure 5).

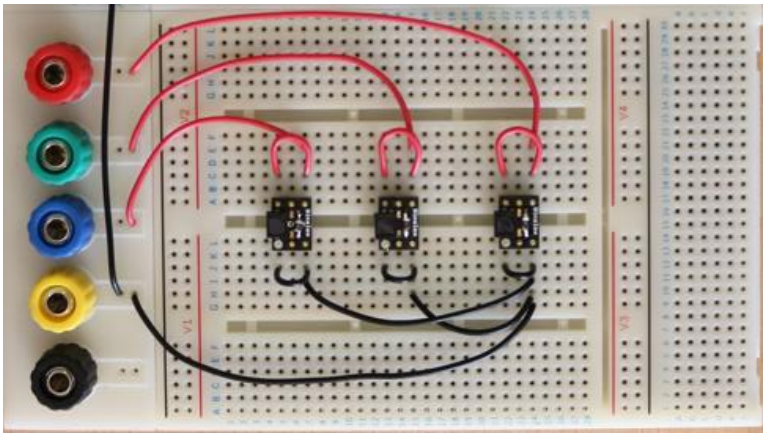

Figure 5: Photodiode electronic test board.

These photodiodes are not adapted for an irradiance of 1000 W/m^2. The saturation occurred at peak days and an optical density has to be considered in order to reduce the solar irradiance in an outdoor measurement. So this problem became too complex to get an acceptable accuracy of the irradiance measurement. Indeed, an additional optical system that reduce the energy received by the PIN photodiode. We can add that the small area of the photodiode can also involve shading problems and complicate electrical connections on a large vehicle roof area.

For all the reasons mentioned, this solution has been cancelled and the solar cells matrix were assumed.

2.2.2 Irradiance matrix detectors with solar cells and temperature sensors

The other solution is to map the roof surface with solar cells. In addition to the simplicity of implementation, it is possible to adapt the reception surface of the illumination. The short-circuit current (I_{sc}) is directly proportional to the irradiance and no temperature dependence is considered. The design of the irradiance detector unit selected is described on Figure 6.

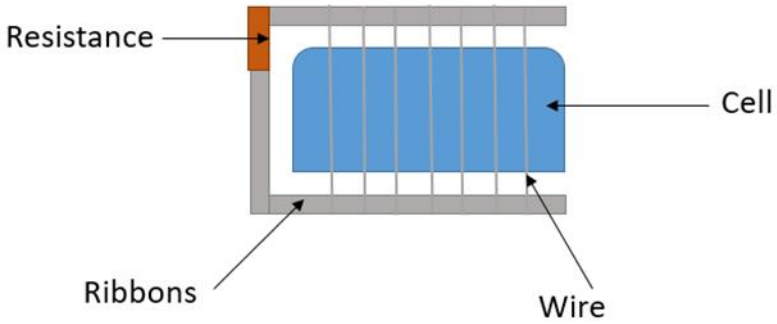

Figure 6: Diagram of connection to ½ M6 solar cell terminals via a low resistance.

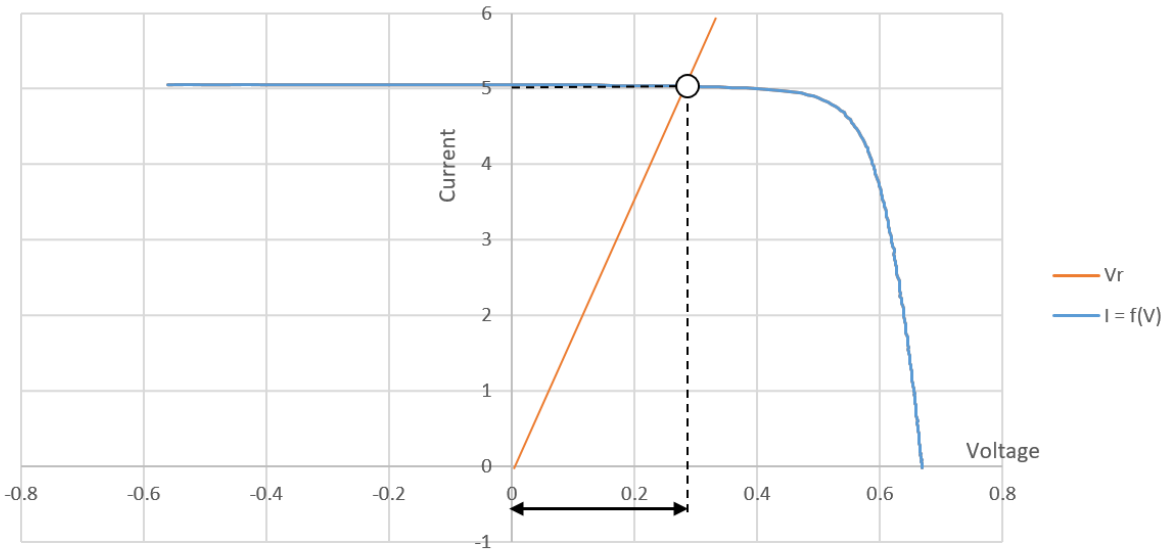

Figure 7: IV curve of the selected cell, with target operating point at 0,3V on current plateau.

A ½ M6 solar cell terminals are connected together with a weak resistance (shunt role) in between. A calculation was made to specify the value of this resistance to set an operative point of this system in the middle of the IV curve, on the plateau (plot in Figure 7). It gives a certain margin to 0 V in term of voltage sensitivity, al also regarding the curve drop close to 0.5 V. We measure with a flash test the IV curve of the selected cell and we chose arbitrary a voltage at 300 mV. With this value, we are able calculate the optimal resistance to add the terminals of our system:

$$V_R = RI$$

With V_R = 0.300 V and I = 5 A (I_{SC})

We obtained a resistance of 60 mΩ. We choose 50 mΩ.

A calibration is needed for every solar cell used for the irradiance matrix. A Xe lamp is available to set the irradiance at 1000 W/m^2 and we measured the voltage at the resistance terminals. This system allows a direct proportional relation between V_r and irradiance.

The specification of the datalogger accepts a maximum of 50 channels. For a better precision, a thermocouple was needed to be set close to the cell in order to control the operating temperature. So, a 5x5 matrix of solar cells and resistance with their thermocouples related are selected. We measured the dimension of the car roof surface: 158 cm x 106 cm. With this information, we decided to split the overall matrix into 5 strips of 5 cells. Each strip measure 140 cm x 15 cm.

The measurement gives a mapping of 25 pixels of the roof with a temperature control at each point. The strips are a lightweight PV module-like structure: we encapsulated the solar cell between polymers. We will specify the bill of materials and the laminating process in the following section. Each output has to be long enough to reach the datalogger placed in a box outside of the irradiance kit (around 2.5 meters wire long). The scheme in Figure 8 describes the complete system scheduled.

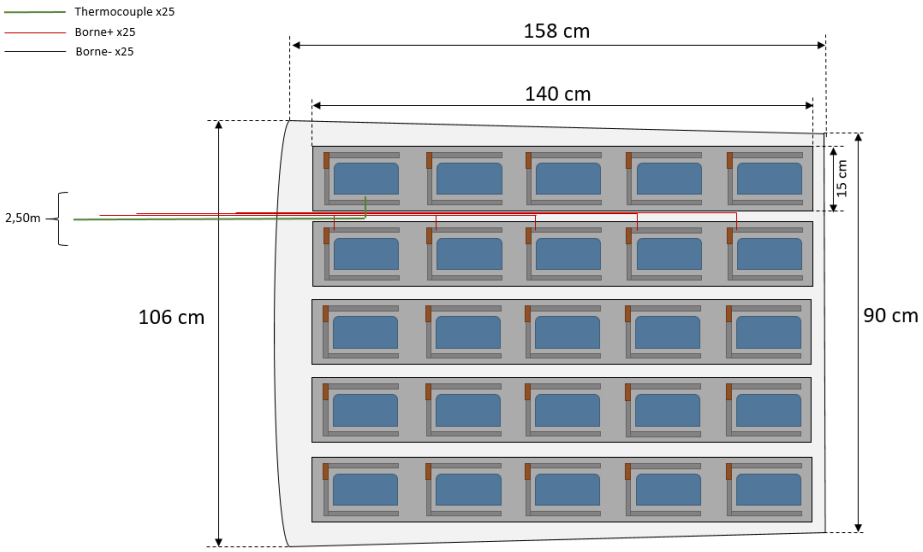

Figure 8: 5 x 5 matrix of solar cells and resistors with their thermocouples.

3- FABRICATION PROCESS

3.1 Electrical component

The solar cell used for this experimentation are M6 PERC solar cell. 9 busbars are set on each side of the cell. Wires are chosen to have a sheath that resists the lamination temperature above 160 °C. PTFE wire sheath was integrated inside the module. This operation point of this material is between -200 °C and 260 °C. For practical use later, the length of these wires should measure around 4m in order to be able to plug it into the datalogger situated around the car roof.

Thermocouple is also chosen to be resistant to lamination temperature. Each thermocouples needed to be wisely set on the module. Indeed, the resistance between ribbons is crossed by around 5A current at 1000 W/m². Therefore, a local temperature rise is predictable around this component. A test measurement has been made before the fabrication in order to get a magnitude of this temperature rising. We measured at 1000 W/m², 70°C around the resistance. Ribbons, wire and thermocouples are brazed with tin without lead.

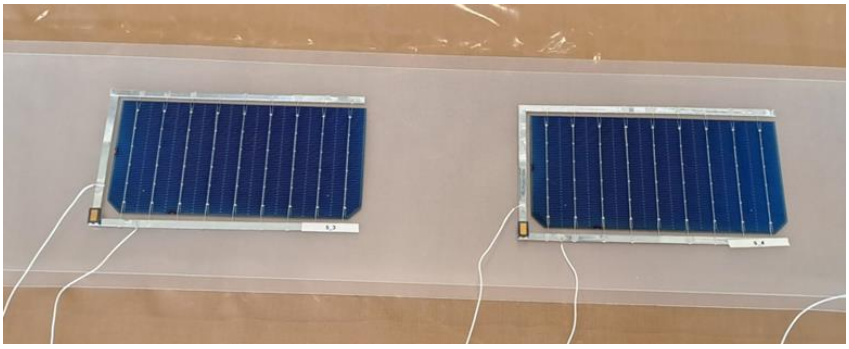

Figure 9: Image illustrating the connection of the wires to the resistor terminals of each cell.

Table 1: Following table summarized the fabrication steps for the irradiance unit:

Step	Operation	Comments
1	Cut the cell wire at an acceptable dimension for brazing	
2	Braze the ribbons to the cell wires	18 brazes in total
3	Braze the perpendicular ribbon to the (-) terminal	
4	Apply tin where the resistance terminal	For easier brazing
5	Weld the resistance	
6	Weld the two wire at each terminal	
7	Label the unit	From 1-1 to 5-5

This operation was repeated 25 times for covering the entire matrix irradiance measurement system.

3.2 Assembling and encapsulation

3.2.1 Choice of materials

The irradiance matrix measurement is similar to a light weight PV module. So, the bill of material is similar to previous studies realized in CEA. The frontsheet and backsheet chosen to be in the module was PET (polyethylene terephthalate) film. Indeed, this polymer has good properties to shield the cells from outdoor environment. It has also a good resistance to thermal cycles and especially good optical properties. Moreover, this PET film is treated with an UV protection. However, this treatment is useless for our purpose because the experiment only lasts one cumulated week. The degradation is not instant. For encapsulant, we chose a thermoplastic olefin. The width of the encapsulant should be greater than the width of the resistance to avoid local constraint due to the overthickness.

The dimension of the different layer is set to 140 cm x 15 cm. It is sufficient to place 5 units of irradiance measurement cells.

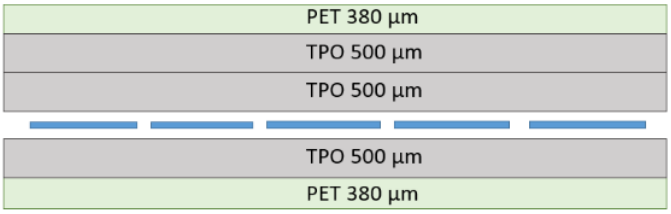

Figure 10: Stacking of selected materials.

3.2.2 Lamination process

Lamination is the process of assembling different layers of materials. The purpose of lamination in the case of photovoltaic module manufacturing is to protect the cells from external contact. The lamination process takes place in several stages. The first steps are assembly with stacking of materials, introduction into the inner chamber of the membrane laminator and application of a lamination recipe.

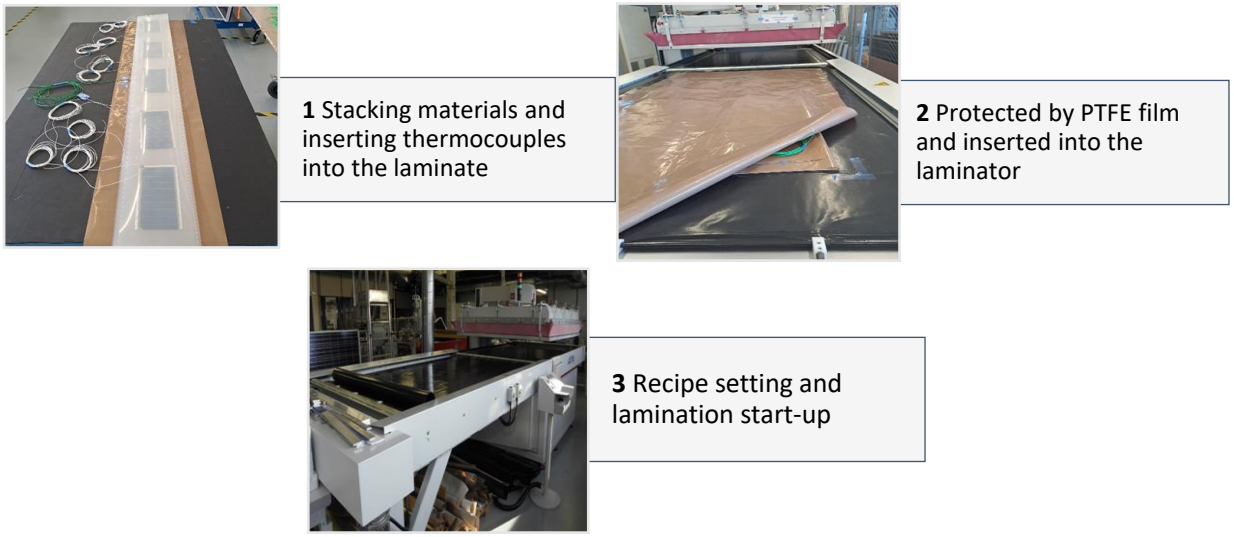

Figure 11: Assembly and introduction of cell strips into the laminator.

The recipe applied to the laminator defines parameters such as temperature and pressure apply. The temperature and pressure conditions allow the cells to be sealed between the two layers of TPO encapsulant and the different faces (front and back) of outer materials to adhere to the encapsulating materials.

Thus, after a first degassing step under pressure at 5 mbar, the laminator reaches a target temperature of 160 °C allowing the encapsulant to reach its melting temperature. To complete the lamination, a cooling step is applied to harden the materials and allow stabilizing the entire module at atmospheric pressure. Cooling is partly done in the open air. The duration of the lamination with this type of module is 17 minutes. The diagram in figure 12 illustrates the different steps in a simplified way.

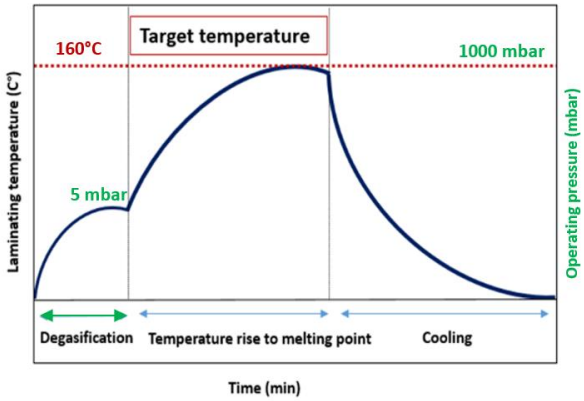

Figure 12: Simplified diagram of lamination steps.

3.3 Measurement bench calibration

The manufacture of irradiance measurement strips is followed by a calibration by a solar simulator. The strips are placed in a room equipped with lamps presented in Figure 13 that reflects light with the same spectral correspondence as natural sunlight. The lighting system of the simulator is composed of 8 luminaires of 4000 W each located at 3 meter above the test bench. It is a complete solar irradiation system to achieve irradiance up to 1100W/m² in the spectral band from 280 nm to 3000 nm in order to be able to perform the sunshine tests according to IEC 61646 and IEC 61215 standards [2]. The lamps used emit a large part of the energy in the spectral band UV, visible and IR.

The different bands of cells were arranged on a bench previously calibrated by the manufacturer [2] with a pyranometer that measures the overall illumination of the test bench. Indeed, as illustrated in Figure 14, we have the assurance of uniformity of illumination at 1000 W/m² +/-5% over the entire surface of the test bench (3000x2000 mm). The calibration consisted in measuring the output voltage at the terminals of the resistors of each cell when they are illuminated by the illumination simulator at 1000 W/m² in a controlled environment.

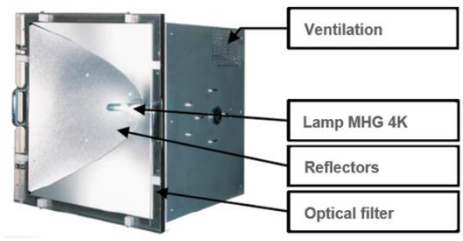

Figure 14 : Composition of solar simulator lamps.

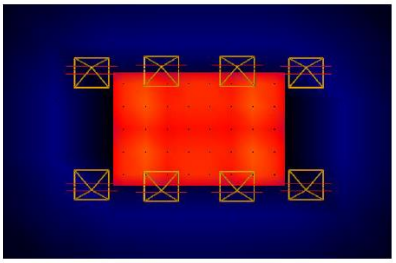

Figure 13 : Illustration of the lamps location on the reference table area.

Figure 15 shows the voltage measurements made from a multimeter on each cell of the matrix bench with the assumption that I_{sc} does not depend on temperature. These values will serve as a reference when processing data obtained during outdoor experiments.

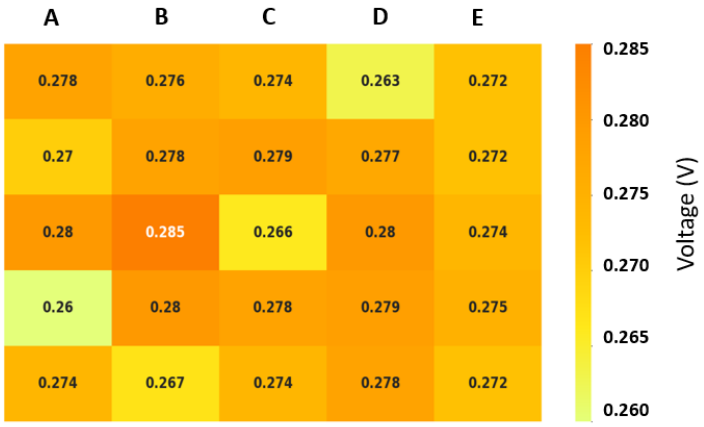

Figure 15: Voltage measurement results for each cell on the solar simulator bench under 1000 W/m².

Each cell is equipped with a thermocouple (type K), calibrated in oven at three different temperatures (30 °C, 50 °C, 70 °C). The standard deviation recorded on 25 thermocouples for each temperature is below 1.5%.

4- INSTALLATION AND SET-UP OF THE MONITORING SYSTEM

4.1 Connection and presentation of the monitoring system

The used data logger shown in Figure 16 is a multi-channel real-time data acquisition system. It is equipped with versatile multiplexers capable of acquiring multiple signals on the same complex communication link. This is a particularly suitable acquisition system for our study with a scan rate capacity of 60 channels/second [3]. As shown in the synthesis diagram, the use of multiplexer makes it possible to simultaneously measure the voltage and temperature of the 25 cells and 25 thermocouples that make up the matrix. With this system, we obtain every minute the value of voltages at the terminals of the resistors as well as the temperature of each of the cells.

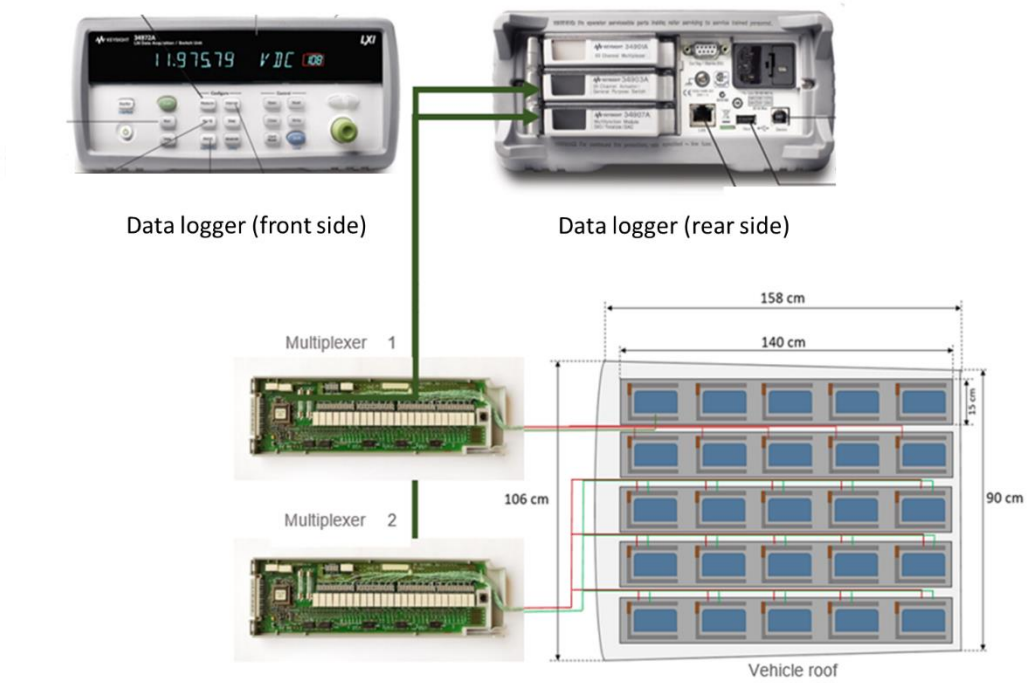

Figure 16: Connection and presentation of the monitoring system.

4.2 Outdoor monitoring and data acquisition

Figure 17 shows the synthesis of the assembly made to obtain the data. After connecting the bench to the data logger, initial tests were carried out via the software of the equipment in the laboratory to ensure the functionality of the data logger.

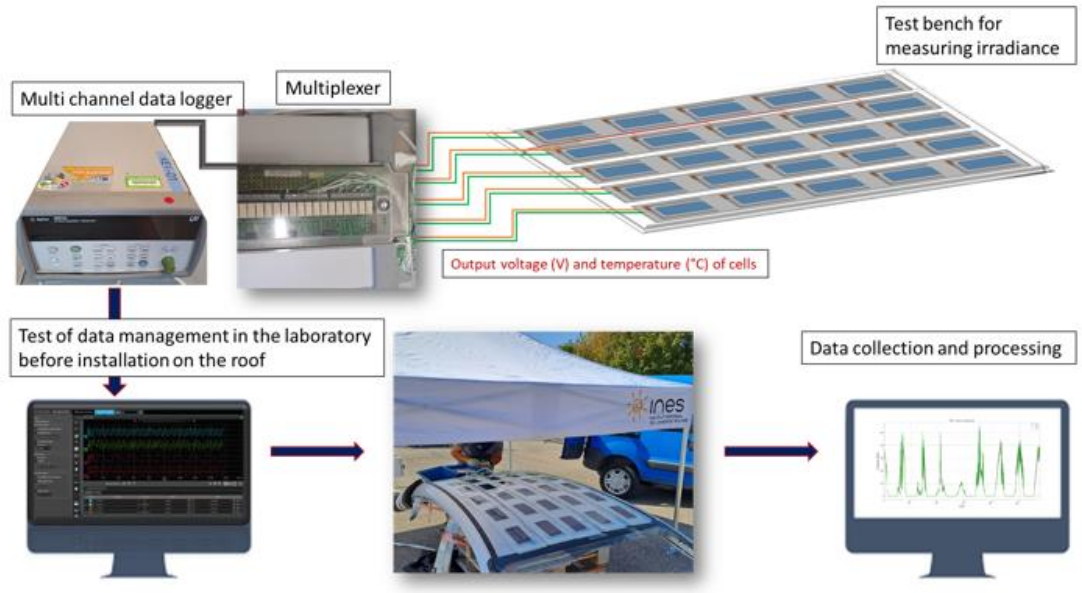

Figure 17: Overview of the irradiance bench set-up used to obtain the data.

After the check, the outdoor installation was done. The roof is divided into 5 strips to fit as close as possible the roof surface. Each strip is in mechanical and thermal contact to the roof surface. The images in Figure 18 show the assembly done outdoors after connection to the data logger and placing strips on the vehicle roof.

Figure 18: Exterior integration of irradiance test bench on vehicle roof.

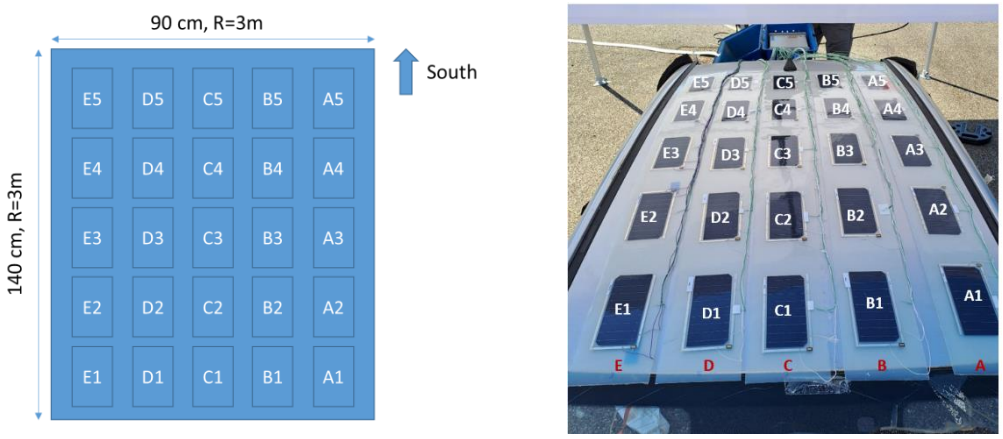

Figure 19 : Left: Top view of the roof with radius of curvature values (R). Right, indexation of cells on the matrix.

The data acquisition took place during 10 consecutive days during the month of August 2023. The objective was to obtain illumination and temperature data in three use cases:

- A hot and clear summer day.

- A cloudy day.

- A rainy day with a temperature below the seasonal norm.

Figure 20 illustrates the irradiance results obtained on cells during the outdoors experiments. It corresponds to the raw data recorded, every minute. The same set of data is recorded in temperature. At this step, it validates that the monitoring system implemented works, with consistent data.

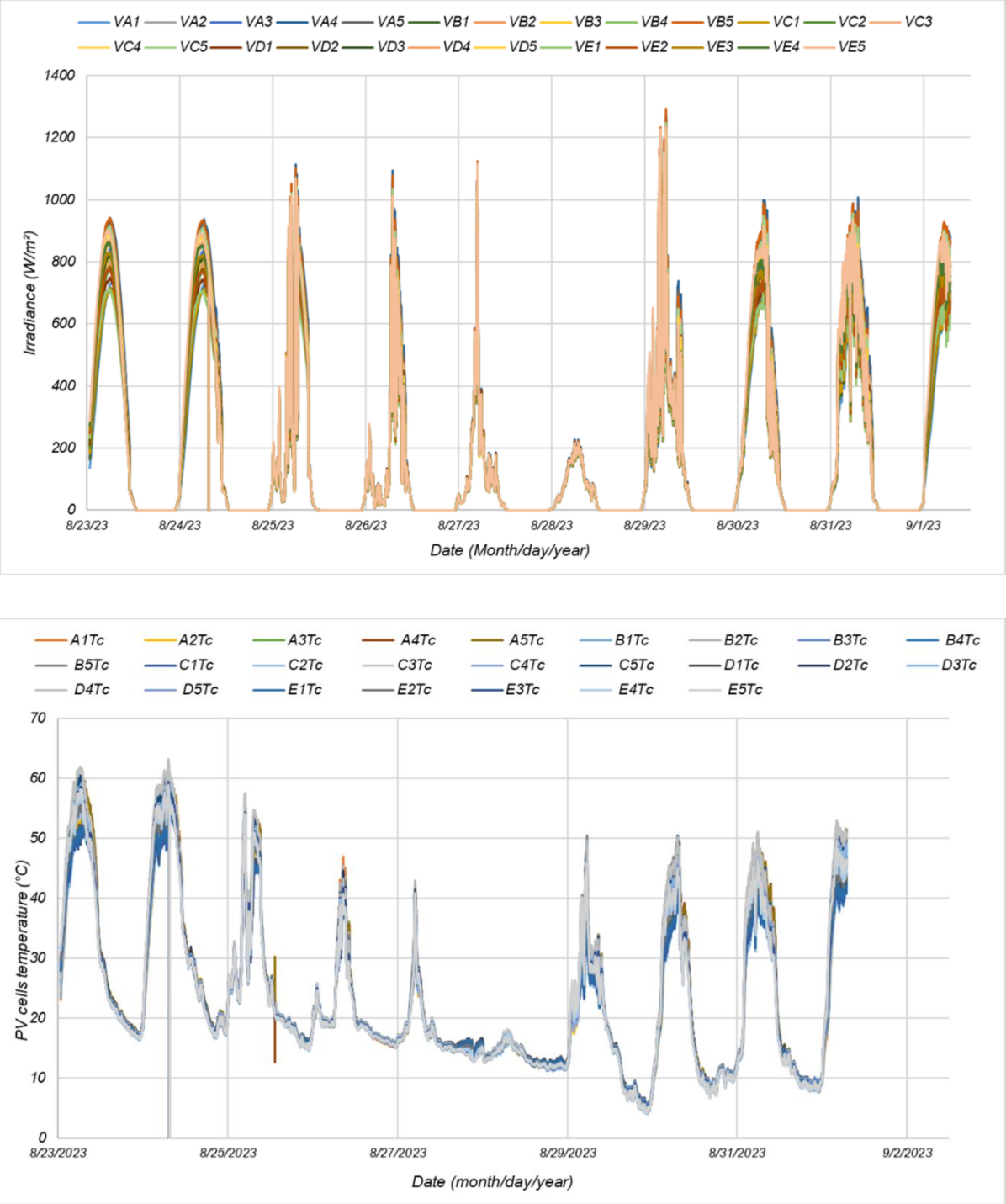

Figure 20: Irradiance and temperature raw data measured on the 25 cells of the matrix.

5- DATA PROCESSING AND PARAMETER EXTRACTION

5.1 Objectives

The main objectives of the test bench are to characterize irradiance and temperature uniformity from data collected from a curved roof of a vehicle during typical summer weathers. This experiment has been setup on an area with no shading in order to record only the influence of the curvature of car roof. The system has been settled on open southern exposition and levelled to be representative of a vehicle random azimuth orientation during parking phase. A correlation is expected between the curvature and the irradiance measurement, and projection could be made with a serial connection of the cells architecture. Three different scenarios are considered:

- One scorching clear summer day.
- One cloudy day.
- One rainy day with temperature below the seasonal norm.

The tests lasted a full week, August 2023 in Bourget du Lac (France). All the three scenarios were available during this week. At the end, this study gives homogeneity values for temperature and irradiance on typical car roof shape. These results will help to project future VIPV modules performances in real operating conditions. This point will be addressed further in the project.

5.2 Parameters calculation

During monitoring phase, global irradiance (G) and temperature (T_{pvcell}) are recorded. These are raw datas. In order to implement these data in VIPV energy prediction model, homogeneity values are extracted. As a first level use case, we consider that every cells are connected in serial connection. It means that a partial shading will results in a global current (and power) limitation of the less exposed cell. To quantify this current limitation, we propose to calculate or extract, at each iteration time, G_{max}, G_{min}, G_{max}-G_{min} over the 25 irradiance sensors matrix. Coupled with an integration time, G is converted in energy (E) to extract energy lost due to irradiance mismatch over time.

Following the same approach, $T_{pvcellmax}$-$T_{pvcellmin}$ gives the temperature amplitude over the entire roof. This value will be considered as an input for a future update of our energy prediction model [4], to calculate thermal induced performances losses for each PV cell, and the consequence at PV module level. Finally, these two informations will be implemented to compare it to the classical approach based on a global percentage energy loss (between 8 to 10% yearly) from an equivalent flat and horizontal PV panel [4].

5.3 Results and discussion

Global irradiance G and cell temperature T_{cell} are plotted respectively in Figures 21 and 22. It focusses on max and min values, to extract amplitudes over 7 entire days on INES site, Le Bourget du Lac (France) during August 2023.

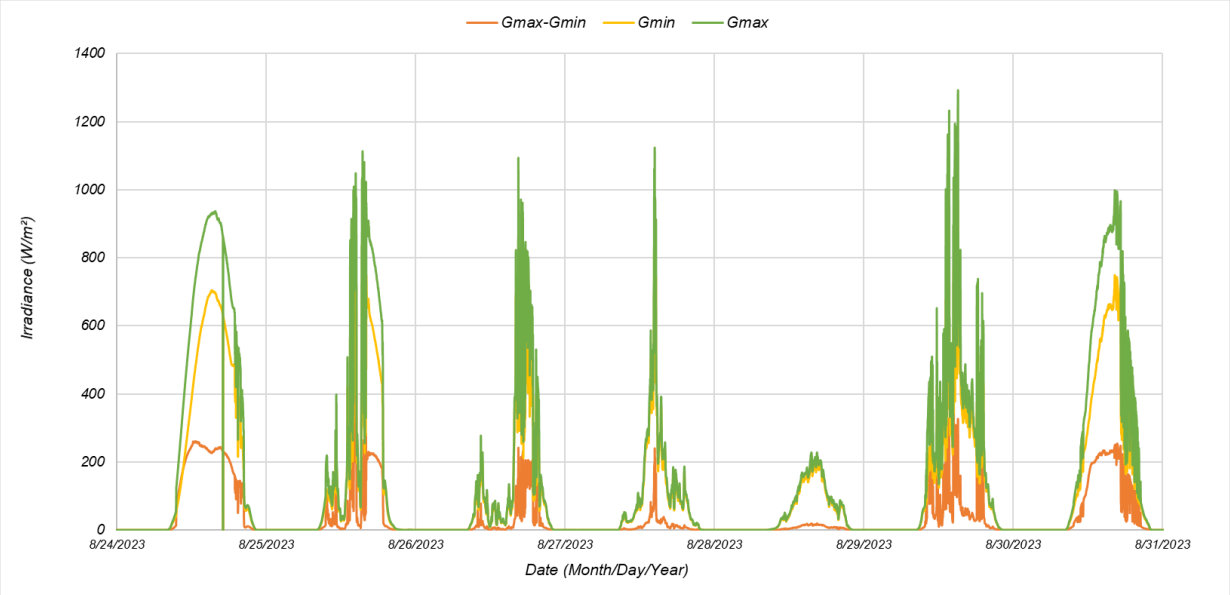

Figure 21: Irradiance data (G_{max}, G_{min}, G_{max}-G_{min} over the entire matrix) recorded on 7 days experiment.

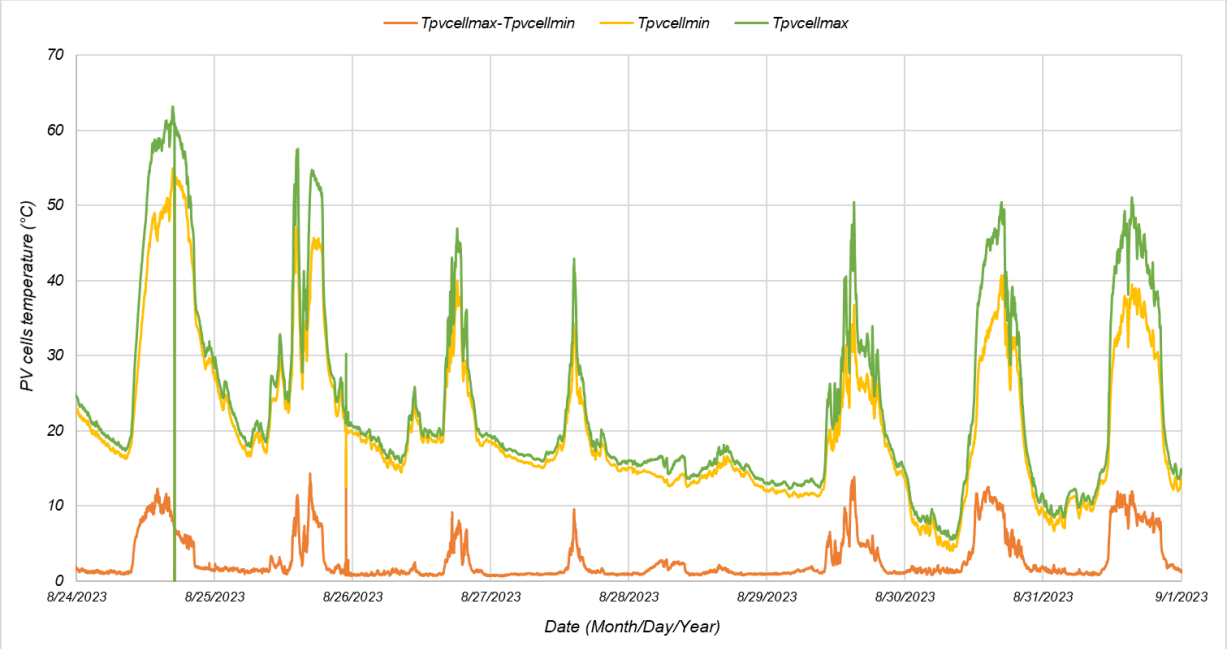

Figure 22: Temperature data (T_{max}, T_{min}, T_{max}-T_{min} over the entire matrix) recorded on 7 days experiment.

Irradiance plot reveals up to 255 W/m² difference between best and worst oriented cell on the roof. Regarding temperature, up to 13 °C difference is confirmed during sunny days. Let's now focus on weather consequences on irradiance and temperature homogeneity.

In Figure 23, Global Irradiances is presented on two different summer weather: scorching clear summer day, and rainy day.

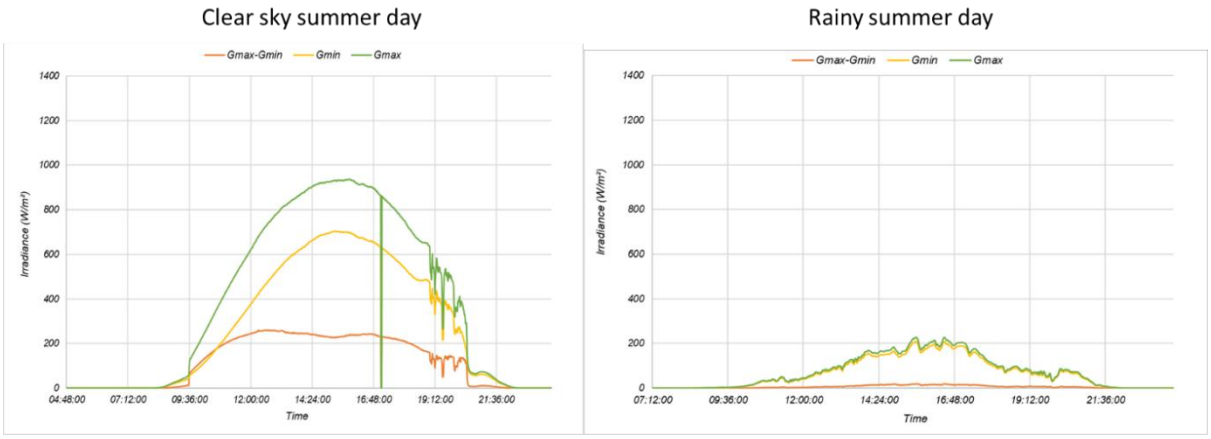

Figure 23: Global Irradiances on two different summer weather: scorching clear summer day (left), and rainy day (Right).

Considering the rainy day conditions, we assume that irradiance is uniform over the matrix and during all day (G_{max}-G_{min} close to 0). Due to a major contribution of diffuse light, every cell collects the same amount of energy without incidence angle differentiation. Now, for the clear sky condition, there is a clear contribution of the angle incidence of each cell against sun elevation. A clear summer day allows to compare the irradiance difference recorded, to the theoretical irradiance assuming the sun elevation and that the direct irradiance is the main light contribution.

During August (on 15th), in Le Bourget du Lac location, the maximum sun elevation is close to 70°. If we consider the geometry and shape of the sensor matrix, the incidence angles are easy to calculate linked to sun elevation. It gives 85° and 55°, respectively for the best and worst irradiance recorded. The situation is described in Figure 24. The irradiance ratio at maximum sun elevation gives 701/930 = 0.75. The same approach with appearance surface gives sin(55)/sin(85) = 0.82. It results in a difference of 9%, which could be explained by specific reflection properties of the sensor matrix, accuracy of the levelling and/or radius of curvature measurement on roof. However, it confirms that the bench works well with coherent results.

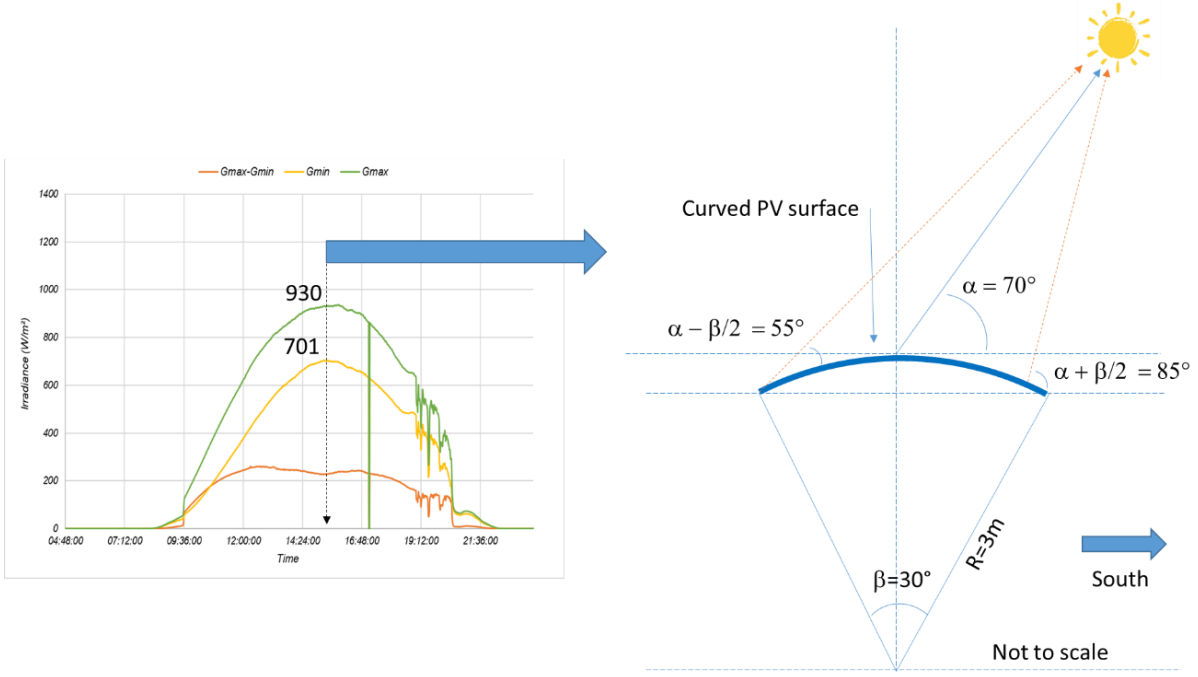

Figure 24: Schematic situation at maximum sun elevation in August, at Le Bourget du Lac, France.

Following the same approach as Figure 23, the equivalent plot for temperature is presented in Figure 25. A 13 °C difference is recorded during a clear sky summer day. We note that PV module structure temperature reaches up to 60 °C. During a rainy summer day, we assume a perfect temperature homogeneity on all module surface.

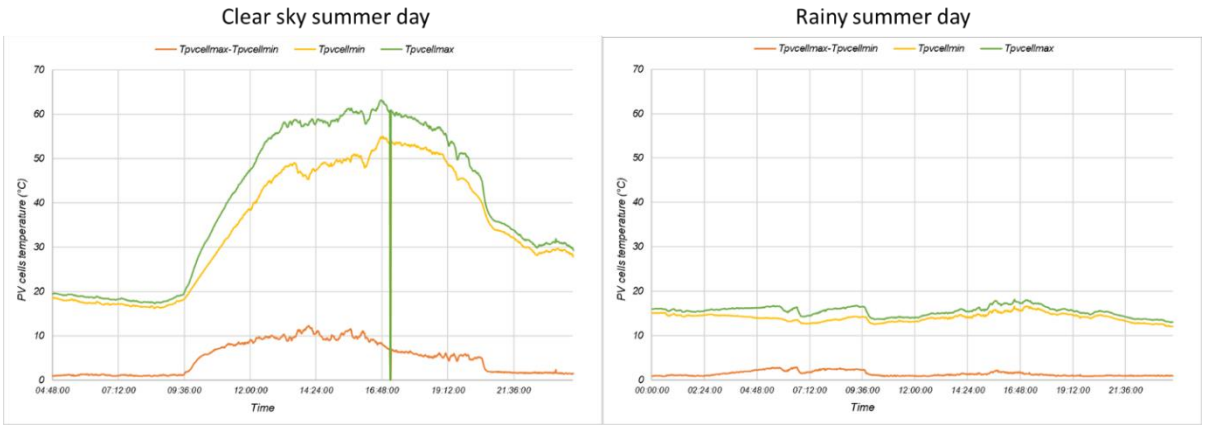

Figure 25: Cells temperature on two different summer weather: scorching clear summer day (left), and rainy day (Right).

Maximum values for Irradiance and cell temperature homogeneity are summarized in Figure 26. It focusses on maximum values only. For a future simulation approach, we propose to consider an irradiance homogeneity at 250 W/m² under 930 W/m², which results in 21% reduction in clear sky summer day, and up to 13 °C cell temperature difference. For a completely summer rainy day, we propose to do not take into consideration temperature and irradiance homogeneity.

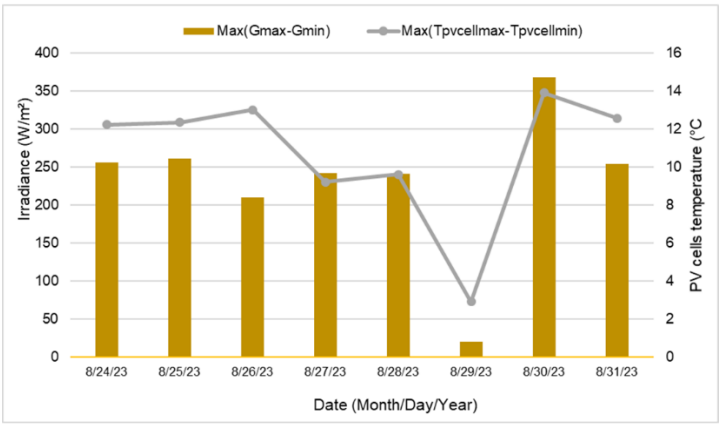

Delta values	Max(Gmax-Gmin) (W/m²)	Max(Tpvcellmax-Tpvcellmin) (°C)
8/24/2023	255,67	**12,22**
8/25/2023	261,04	**12,33**
8/26/2023	210,00	**13,00**
8/27/2023	242,07	**9,19**
8/28/2023	240,16	**9,59**
8/29/2023	19,58	**2,89**
8/30/2023	367,27	**13,89**
8/31/2023	254,07	**12,55**

Figure 26: Maximum values for irradiance homogeneity and cell temperature on solar roof over experiment time. It focuses only on maximum values.

We now propose to translate irradiance values into energy to project energy harvesting values, and losses due to irradiance mismatches with roof curvature. Linked to the hypothesis explained before, and as a first level use case, we consider that every cells are connected in serial connection in a standard VIPV module. It means that a partial shading or irradiance mismatch will results in a global current (and power) limitation of the less exposed cell.

We propose to calculate the following parameter:

- **E** $_{\text{all PV cell}}$: Energy mean value (kWh/m²) over the entire roof. For each PV sensor, the irradiance value is integrated over time, every minute. It results on one value per cell, and a mean value is calculated on the 25 PV sensors.
- **E** $_{\text{pvcells max}}$: Every minute, the maximum irradiance value from the matrix is considered for energy calculation. At the end it overestimates the energy harvested by the entire roof.

- **E $_{pvcells\ min}$**: every minute, the minimum irradiance value from the matrix is considered for energy calculation. At the end, the value aims to be representative of a real curved PV module with a power limitation by the less exposed cell (every cells in serial connections).

These three parameters are summarized in Figure 27, with detailed values, and final differences between $E_{pvcell\ min}$ and $E_{all\ pvcells}$ in percent. It gives between 12% and 17% for clear sky summer day, and 6% only during a rainy summer day.

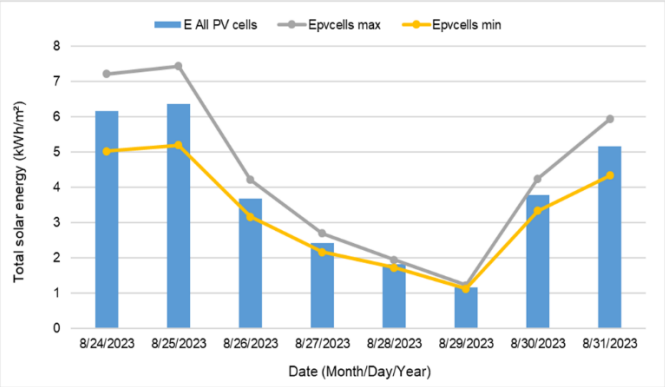

kWh/m²	E All PV cells	Epvcells max	Epvcells min	E all pv cells-Epvcells min	E all pv cells-Epvcells min (%)
8/24/2023	6,16	7,21	5,02	1,06	**17%**
8/25/2023	6,36	7,43	5,19	1,07	**17%**
8/26/2023	3,68	4,21	3,17	0,52	**14%**
8/27/2023	2,41	2,69	2,16	0,28	**12%**
8/28/2023	1,82	1,94	1,72	0,12	**7%**
8/29/2023	1,16	1,22	1,12	0,07	**6%**
8/30/2023	3,78	4,24	3,33	0,46	**12%**
8/31/2023	5,15	5,93	4,33	0,79	**15%**

Figure 27: Energy calculation values in kWh/m² considering all cells (roof average), the best exposed cell propagated over entire roof, and the worst exposed cell propagated over entire roof.

6- CONCLUSION

This report illustrated the various stages in the implementation of a measurement bench, from design, installation, monitoring phase and data processing. We were thus able to develop a sensor matrix (5x5) for measuring solar irradiance on a vehicle roof, with temperature sensors. The test bench was placed on open southern exposition and levelled to be representative of a vehicle random azimuth orientation during parking phase. Data have been recorded during 8 days, during August 2023, at INES site, Le Bourget du Lac, France.

A simple theoretical comparison confirmed that irradiance and temperature uniformity is mainly due to roof curvature. For clear sunny days, Irradiance data reveals up to 250 W/m² (21%) difference between best and worst oriented cell on the roof. Regarding temperature, up to 13 °C difference is confirmed. For rainy days, we found less than 20 W/m² irradiance difference and less than 3 °C temperature homogeneity. Thus, we propose to consider irradiance and temperature mismatches only on clear sky conditions (direct irradiance as main energy contribution). Energy calculations coupled with a full serial cells connection hypothesis and a curved surface (Radius of curvature =3 m) show that the energy harvesting is limited by 12 to 17% performance loss on clear sky sunny day, and 6% for rainy days. These values are valid for August only. This study should be done on one year duration.

Further steps will focus on energy model prediction at vehicle level (irradiance and temperature mismatch versus standard “x” % losses approach) to quantify the accuracy/complexity of both approaches. Another interesting work should be to install again this bench over a year to duplicate this study, every month. These steps should be addressed in a couple of years.

REFERENCES

[1] Silicon PIN Photodiode Vishay ref: VEMD5080X01 www.vishay.com

[2] Atlas material testing solutions-Instruction manual solar constant 4000

[3] Jin - 34970A Data AcquisitionSwitch Unit Family-Technical overview Keysight

[4] Karoui, Fathia, Bertrand Chambion, Fabrice Claudon, and Benjamin Commault. 2023. "Integrated Photovoltaics Potential for Passenger Cars: A Focus on the Sensitivity to Electrical Architecture Losses" Applied Sciences 13, no. 14: 8373. https://doi.org/10.3390/app13148373